LAUTECH Journal of Engineering and Technology 17 (1) 2023: 83-95

FREQUENCY AND VOLTAGE RESPONSES OF GAS-FIRED DISTRIBUTED GENERATION SYSTEM TO LOAD CHANGES UNDER STAND-ALONE AND GRID-CONNECTED MODES

[1]Adedokun, J. L., [1]Adejumobi, I. A, [1]Adebisi, O. I and [2]Olajuwon, B. I.

[1]Department of Electrical/Electronics Engineering, Federal University of Agriculture, Abeokuta, Nigeria.
[2]Department of Mathematics, Federal University of Agriculture, Abeokuta, Nigeria.
Corresponding Author: engradejumobi@yahoo.com

ABSTRACT

Research has shown that addition of loads to a distributed generation (DG) system operating either in stand-alone mode (SAM) or grid-connected mode (GCM) has impacts on its operations. This paper analyzed the voltage and frequency responses of the DG when operated in stand-alone and grid-connected modes under load variations. Mathematical equations showing the characteristics of the DG under varying loads with the two modes were developed. The equations were modeled using MATLAB in Simulink environment. By applying gradual and sudden loads using 2MW DG and an 11kV distribution grid network, the frequency and voltage responses under the two modes were calculated. The results showed that with gradual load addition from 10 to 100 % loading, the output frequency varied from 49.72 to 49.27 Hz (-0.56 to -1.46 %) for SAM while it varied for GCM from 49.90 to 49.44 Hz (-0.20 to -1.12 %). Output voltage varied from 376 to 232.9 V (-6.0 to -41.78 %) for 10 to 100 % load respectively for SAM while it varied from 387.7 to 268.3 V (-3.08 to -32.93 %) for GCM. For sudden load additions, the output frequency variation was between 49.39 to 49.25 Hz (-1.22 to -1.5 %) for 25 to 100 % load for SAM while that of GCM was between 49.51 to 49.43 Hz (-0.98 to -1.14 %); voltage variation was 271.7 to 190 V (-32.08 to -52.5 %) for 25 to 100 % load respectively for SAM while that of GCM was 294.2 to 219.9V(-26.45% to -45.03%). The results revealed that the frequency with gradual and sudden load additions for SAM and GCM varied outside the operational limit of 49.75-50.25 Hz (± 0.5 %) except in the case of 10 % load under gradual load addition in GCM. However, the frequency and voltage variation are less in GCM than SAM with gradual and sudden load additions

Keywords: *Distributed generation; modelling; simulation; stand-alone mode; grid-connected mode; comparative analyses; frequency and voltage responses.*

INTRODUCTION

Modern civilization and day to day electric power demand has led to the increase in the demand of electrical energy for residential, commercial and industrial applications (Esan *et al.*, 2019). Electrical energy in the years past has been generated in Nigeria by centralized power system which make use of thermal power plants, hydro power plants, nuclear power plants, etc. (Simeon *et al.*, 2018). However, this centralized generation of power has some challenges which include inaccessibility of some rural areas to electricity, losses of electrical power as a result of long transmission and distribution lines, high cost of upgrading the transmission and distribution system to meet up with increasing energy demand etc. (Kabalci *et al.*, 2021). These challenges have led to a shift towards an alternative power generating system known as distributed generation system (Oladipo *et al.*, 2018). The distributed generation (DG) involves electricity generation at the level of distribution which is the closest voltage level of electric power supply system

to the consumers (Agbetuyi *et al.*, 2021). The merits of distributed generation include frequency and voltage enhancement, power loss mitigation, efficiency improvement, system reliability improvement as well as reduction of operational and maintenance costs (Samala and Kotapuri, 2018). Several of electric power networks nowadays are operating as DG models connected with non-renewable and renewable energy power plants to form a microgrid (Kim *et al.*, 2019). A microgrid can either operate in stand-alone mode or grid-connected mode (Mahmoud *et al.*, 2023). Researchers have found that addition of loads to the distributed generation system during its operations in any of these modes have effects on the operational frequency, voltage and power flow of the system which impacts on the stability of the system and hence, the need to carry out this study on the analyses of the responses of distributed generation system operating in stand-alone and grid-connected modes when load changes.

LITERATURE REVIEW

Rudresha *et al.* (2020) worked on the effects of connection of distributed generation (DG) system to distribution network for mitigation of loss and voltage stability under various loading conditions. It proffered a means of choosing the right location and size of the DG to be connected to the distribution network as a way of reducing the losses and enhancing the voltage stability under various loading conditions. Power World Simulator was used as a software to simulate IEEE 33-Bus system while the resulting power losses and voltage profile were analyzed. The results showed that choice of the right location and size of the DG helped to reduce the system losses and boost the voltage profile and hence enhance the system voltage stability.

Investigation of the effects of DG integration on the transient stability and small-signal stability of the system for unequal and equal load increase conditions was carried out by Patil *et al.* (2021). The scenario of unequal load increase was simulated with the use of orthogonal array. The effect of DG integration on small-signal stability was analyzed with the use of critical eigenvalues while the transient stability was analyzed using time-domain indicators. Synchronous generator was used to interface micro turbine generator and diesel turbine generator as DG sources with wind turbine generator. The result showed that the power system displayed various stability responses for unequal and equal load increase conditions for a single DG load.

The technical characteristics of distributed generation was analyzed by Zhang *et al.* (2023). It also analyzed the effects of distributed generation on the voltage of the grid distribution network from the point of view of capacity and position. It concluded that the capacity, connected position and the type of distributed generation control the impact of the distributed generation on the existing distribution network voltage. It pointed out that further research can be carried out in the area of renewable energy based distributed technology to help power system more.

Salimon *et al.* (2023) worked on the effects of the level of penetration of DG on the voltage profile and power loss of the radial distribution systems using various forms of DG. The real and the reactive powers injected by the different forms of DG were used as basis for modeling those forms of DG. Voltage profile index was utilized to compare the voltage profiles gotten in different scenarios. The voltage profile index gives a magnitude to show how close the voltages are to the ideal voltage. Identification of the most sensitive buses for integration of the DG was achieved using two power voltage stability indices.

Sule (2022) examined the challenges posed by the integration of renewable energy sources to location of fault, system stability and fault protection. The effect of renewable energy sources on location of

fault was tackled using knowledge-based approaches. The effect of renewable energy sources on protection schemes was deduced using optimized and programmed relays while the effect of renewable energy sources on system stability was solved using Virtual DGs.

This paper analyzed the frequency and voltage responses of a DG system in both SAM and GCM. Comparison was then made between the voltage and frequency responses of SAM and GCM after which it was concluded that operating a DG system in GCM is better than in SAM due to lesser variations in frequency and voltage when load is added to the system.

METHODOLOGY

The equations describing the frequency, voltage and power on the DG system in stand- alone and when it is grid connected modes are provided in this section. Mathematical equations that described the characteristics of the DG under varying loads with the two modes were developed. The equations were modeled using MATLAB 2018a in Simulink environment. By applying gradual and sudden loads using 2MW DG and an 11kV distribution grid network, the frequency and voltage responses under the two modes were calculated. The results were then analysed and appropriate conclusions were made based on the obtained results and related standards by the Nigeria Electricity Regulatory Commission (NERC).

Dynamics of a Synchronous Machine

The equations governing the dynamics of a synchronous machine are given by eqns. (1) to (7).

For a synchronous machine, the kinetic energy (KE) of the rotor is given by eqn. (1)

$KE = \frac{1}{2} J w_{sm}^2 10^{-6}$ (Kothari and Nagrath, 2009) (1)

Where J is the rotor moment of inertia in kg-m^2, w_{sm} is the synchronous speed in rad (mechanical)/sec.

But w_{sm} is given by eqn. (2)

$w_{sm} = (\frac{2}{P}) w_{se}$ (Kothari and Nagrath, 2009) (2)

Where w_{se} is defined as the rotor speed in electrical rad (electrical)/sec and p is the number of poles of the machine.

Putting eqn. (2) in eqn. (1) gives eqn. (3)

$KE = \frac{1}{2} (J(\frac{2}{P})^2 w_{se} \times 10^{-6}) w_{se}$ MJ (3)

From eqn. (3),

$J(\frac{2}{p})^2 * w_{se} * 10^{-6} = M$ (4)

Where M is the is the moment of inertia in MJ

Inertia constant H(in MJ/MVA or MW − sec/ MVA) is defined such that

$GH = KE = \frac{1}{2} M w_{se}$ (5)

Where G is the three phase MVA rating of machine.

Manipulating eqn. (5) yields

$M = \frac{2G}{w_{se}} = \frac{2GH}{2\pi f} = \frac{GH}{\pi f}$ MJ. sec/elect. rad ($\because w_{se} = 2\pi f$) (6a)

Where f is the rotor frequency in Hertz.

or

$M = \frac{GH}{180f}$ MJ. sec/elect. degree ($\because 2\pi\, rad = 180\, degrees$) (6b)

Taking G as base, M in pu is given as

$M_{(pu)} = \frac{H}{\pi f} sec^2/elect.\, radian$ (7a)

or

$M_{(pu)} = \frac{H}{180f} sec^2/elect.degree$ (7b)

The swing equation

For a synchronous machine, the differential equation governing the rotor dynamics is given as

$J w_{sm} \frac{d^2\theta_m}{dt^2} \times 10^{-6} = P_m - P_e \quad MW$

(Kothari and Nagrath, 2009) (8)

Where P_m is the input mechanical power in MW, P_e is the output electrical power also in MW,

θ_m is angle in rad (mech)

Putting (2) in (8) yields (9)

$\left(J\left(\frac{2}{P}\right)^2 w_s \times 10^{-6}\right) \frac{d^2\theta_e}{dt^2} = P_m - P_e \quad MW$

Or $M\frac{d^2\theta_e}{dt^2} = P_m - P_e \quad MW$ (9)

Where θ_e is angle in rad (elect)

It is easier to measure the angular position of the rotor with respect to a synchronously rotating frame of reference. Assume

$\delta = \theta - w_s t$ (10)

Where δ is the rotor angular displacement from synchronously rotating frame of reference

Which is also known as power angle or torque angle.

Differentiating (10) twice yields

$\frac{d^2\delta}{dt^2} = \frac{d^2\theta_e}{dt^2}$ (11)

Putting (11) in (9) yields

$M\frac{d^2\delta}{dt^2} = P_m - P_e \quad MW$ (12)

Putting (6) in (12) gives

$\frac{GH}{\pi f}\frac{d^2\delta}{dt^2} = P_m - P_e \quad MW$ (13)

Dividing both sides of (13) by G (which is the MVA rating of the machine) yields

$M_{(pu)}\frac{d^2\delta}{dt^2} = P_m - P_e \ pu$ (14)

Where $M_{(pu)} = \frac{H}{\pi f}$

Or

$\frac{H}{\pi f}\frac{d^2\delta}{dt^2} = P_m - P_e \ pu$ (15)

Equation (15) is the "Swing Equation", which is used to describe the dynamic performance of the distributed generation under steady and transient conditions.

Change of frequency of the stand-alone system

Whenever the input mechanical power (P_m) and the output electrical power (P_e) are equal, the system frequency remains unchanged. If P_m is greater than P_e the frequency increases while the frequency decreases when P_m is less than P_e. This shows that the frequency depends on the torque balance since power depends on the torque. Therefore, the torque balance equation of a generator is given in eqn. (16)

$T_i - T_e = J\frac{d\omega}{dt}$ (16)

T_i is turbine torque in Nm and T_e is the electromagnetic torque also developed in Nm.

For a generator, the inertia constant (H) can be expressed as in eqn. (17)

$H = \frac{\frac{1}{2}J\omega_{sm}^2}{S_r}$ MWs/MVA (Hayerikhiyavi and Dimitrovski, 2021) (17)

Where S_r is the MVA base rating of the generator.

From eqn. (17),

$J = \frac{2HS_r}{\omega_{sm}^2}$ (18)

Inserting eqn. (18) in eqn. (16) yields

$T_i - T_e = \frac{2HS_r}{\omega_{sm}^2}\frac{d\omega}{dt}$ (19)

By making $\frac{d\omega}{dt}$ as the subject of the formular in eqn. (19), we have

$\frac{d\omega}{dt} = \frac{\omega_{sm}^2}{2HS_r}(T_i - T_e)$ (20)

In power system, the most appropriate way to express quantities is in per unit form. Therefore, eqn. (20) can be written in per unit form as shown in eqn. (21)

$\frac{d\omega}{dt} = \frac{(P_m - P_e)}{2H}$ (21)

Therefore, change of frequency ($d\omega$) can be expressed as

$d\omega = \frac{(P_m - P_e)}{2H}dt$ (22)

Or

$d\omega = \frac{\Delta P}{2H}dt$ (23)

Where

$\Delta P = P_m - P_e$ (24)

ΔP is the change in power.

Eqn. (23) is the change of frequency equation which shows that the change of frequency depends on the change in power (ΔP) and the inertia constant(H).

Change of voltage of the stand-alone system

The expression for the generator's change in voltage can be determined from the power flow formular

$P_e = \frac{|E||V|}{X_T}\sin\delta$ (Saadat, 1999) (25)

Where P_e is as defined before

|E| is the modulus of the generator's induced voltage in V,

|V| is the modulus of the terminal voltage in V,

X_T is the Power Transfer reactance in Ω.

δ is load angle in degree

if $\delta = 90°$, equation (25) becomes

$$P_e = \frac{|E||V|}{X_T} \quad (26)$$

Since $\sin 90° = 1$

Making |V| the subject of the formula in (26), we have

$$|V| = \frac{P_e X_T}{|E|} \quad (27)$$

Synchronous generator model

The model is a sixth-order state-space model considering the dynamics of the stator, field, and damper windings. The equivalent circuit of the model is represented in the rotor reference frame (qd frame). The rotor parameters and electrical quantities are viewed from the stator. The equivalent circuits are shown in Figure 1.

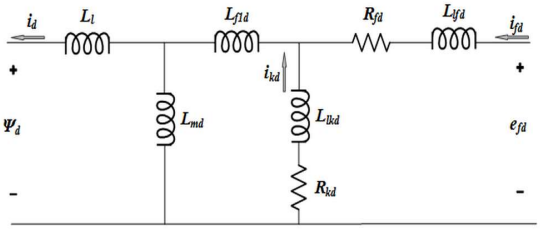

(a)

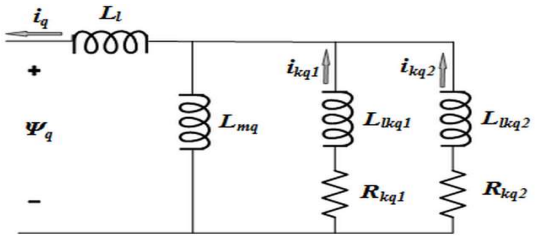

(b)

Figure 1: Equivalent circuits for the synchronous generator

(a) Direct axis (d-axis)

(b) Quadrature axis (q-axis)

Synchronous machine equations can be simplified should the phase variables be transformed from stationary coordinate system a, b, c to the corresponding rotating d, q system (as shown in Figure 1) which is otherwise known as park transformation. This transformation produces eqns. (28) to (34) (Shokooh, 1979).

$$V_d = -i_d R_s - \omega\psi_q + \frac{d\psi_d}{dt} \quad (28)$$

$$V_q = -i_q R_s - \omega\psi_d + \frac{d\psi_q}{dt} \quad (29)$$

$$V_o = -i_o R_o + \frac{d\psi_o}{dt} \quad (30)$$

$$V_{fd} = \frac{d\psi_{fd}}{dt} + -R_{fd} i_{fd} \quad (31)$$

$$0 = \frac{d\psi_{kd}}{dt} + R_{kd} i_{kd} \quad (32)$$

$$0 = \frac{d\psi_{kq1}}{dt} + R_{kq1} i_{kq1} \quad (33)$$

$$0 = \frac{d\psi_{kq2}}{dt} + R_{kq2} i_{kq2} \quad (34)$$

The flux linkages are related to the currents by eqns. (35) and (36)

$$\begin{matrix}\psi_d \\ \psi_{kd} \\ \psi_{fd}\end{matrix} = \begin{bmatrix} L_{md} + L_1 & L_{md} & L_{md} \\ L_{md} & L_{lkd} + L_{f1d} + L_{md} & L_{f1d} + L_{md} \\ L_{md} & L_{f1d} + L_{md} & L_{lfd} + L_{f1d} + L_{md} \end{bmatrix} \begin{matrix}-i_d \\ i_{kd} \\ i_{fd}\end{matrix} \quad (35)$$

$$\begin{matrix}\psi_q \\ \psi_{kq1} \\ \psi_{kq2}\end{matrix} = \begin{bmatrix} L_{mq} + L_1 & L_{mq} & L_{mq} \\ L_{mq} & L_{mq} + L_{kq1} & L_{mq} \\ L_{mq} & L_{mq} & L_{mq} + L_{kq2} \end{bmatrix} \begin{matrix}-i_q \\ i_{kq} \\ i_{kq2}\end{matrix} \quad (36)$$

Where d, q is axis quantity, R *and* S are rotor and stator quantity respectively, L *and* m are leakage and magnetizing inductance respectively, f *and* k: Field and damper winding quantity respectively and ψ is the flux linkage.

The governor system

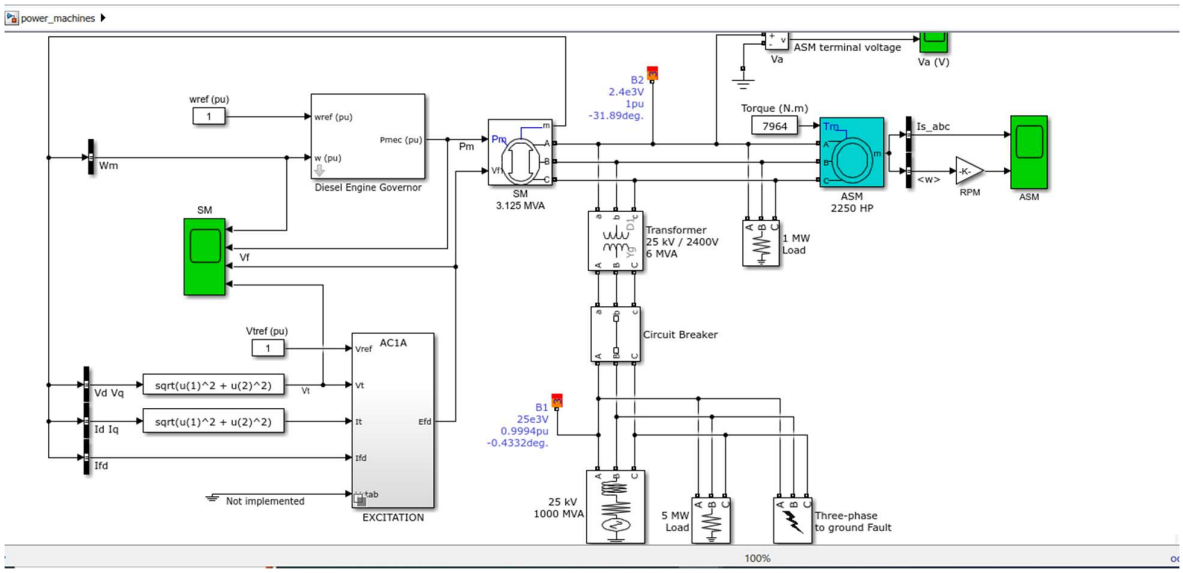

Figure 2: MATLAB-Simulink governor model of a diesel generator

The model in Figure 2 is the MATLAB-Simulink model of a diesel generator which contains the governor system used in this work. The governor system consists of a regulator represented by the following transfer function

$$Hc = \frac{K(1+T3(s)}{(1+T1(s)+T1.T2(s^2))} \quad (37)$$

The throttle actuator is implemented as

$$Ha = \frac{(1+T4(s)}{[(s(1+T5(s)(1+T6s)]} \quad (38)$$

Where K is the regulator gain while T3, T1, and T2 are regulator time constants

Excitation system model

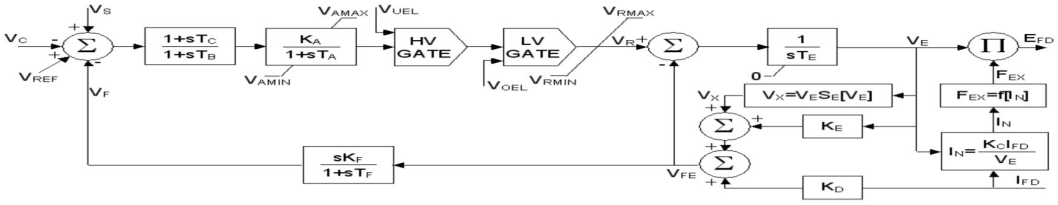

Figure 3: IEEE AC1A excitation system

Figure 3 is the IEEE AC1A excitation system. This block models an ac alternator driving a diode rectifier to produce the field voltage V_f required by the synchronous machine block. A non-controlled voltage regulator provides a voltage in p.u. with a lower limit of zero imposed by the diode rectifier. The exciter does not employ self-excitation, and the voltage regulator power is taken from a source that is not affected by external transients. The diode characteristic in the exciter output imposes a lower limit of zero on the exciter output voltage.

I_{FD} is the demagnetizing effect of load current, V_E is the output voltage, $K_D, K_{c,} K_A K_E$ are feedback constants and E_{FD} is the exciter output voltage.

Frequency for the grid-connected mode

For a DG integrated power system, swing equation can be written as

$$\frac{H}{\pi f}\frac{d^2\delta}{dt^2} = P_m - P_{max}\sin\delta - D\frac{d\delta}{dt} \quad \text{(Chuvychin } et \text{ } al.\text{, 2008)} \quad (40)$$

But $P_m - P_{max}\sin\delta - D\frac{d\delta}{dt} = \Delta P$ (40a)

Where D is the load damping constant, P_{max} is the carrying capacity of the transmission line in MW and other parameters remained as previously defined.

From eqns. (15) and (24),

$$\frac{H}{\pi f}\frac{d^2\delta}{dt^2} = P_m - P_e = \Delta P \quad (41)$$

Eqn. (23) can be modified for grid-connected mode by substituting eqn. (40a) into eqn. (23) to give eqn. (42)

$$d\omega = \frac{P_m - P_{max}\sin\delta - \frac{d\delta}{dt}}{2H}dt \quad (42)$$

Voltage for the grid-connected mode

Just like for the stand-alone system, the voltage for the grid-connected system can be determined as follows.

$$P_{12} = \frac{V_1 V_2}{X_{12}}\sin\theta \quad \text{(Kow } et\ al.\text{, 2015)} \quad (43)$$

Where P_{12} is the real power flowing from the DG to the grid in MW, V_1 is the DG voltage in V,

V_2 is the grid voltage in V and θ is the power angle in degrees.

Modelling of the system in MATLAB in SIMULINK environment

The DG system both in stand-alone and grid-connected modes were modelled in MATLAB in Simulink environment. The stand-alone model in Figure 4 consists of a 2MW test natural gas-based distributed generator whose operating voltage and frequency were 400V and 50Hz respectively, an excitation system for voltage regulation and a governor for voltage regulation. The grid-connected model in Figure 4 consists of the same components as the stand-alone model and a distribution network to which the DG was connected.

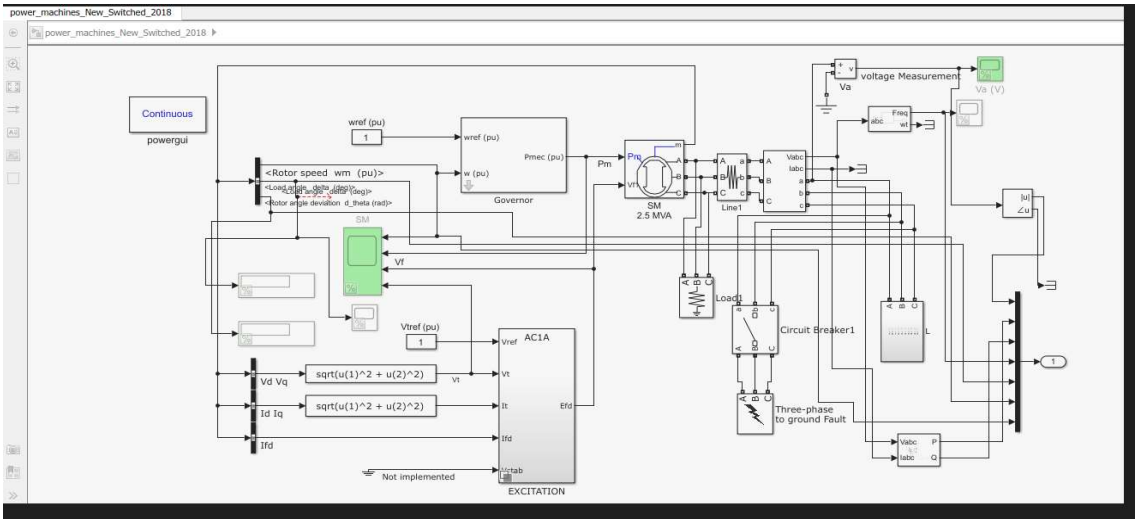

Figure 4: Model of the stand-alone distributed generation system.

RESULTS AND DISCUSSION

The results obtained for the frequency and voltage responses of the DG system operating in stand-alone and grid-connected modes were presented and analyzed in this session. For both gradual and sudden load additions in SAM and GCM, the responses were obtained by running the system on no load for 5 seconds before loads were applied.

Frequency responses with gradual load addition

The frequency responses of the distributed generation system SAM and GCM to the gradual load addition are shown in Figures 6a and 6b respectively.

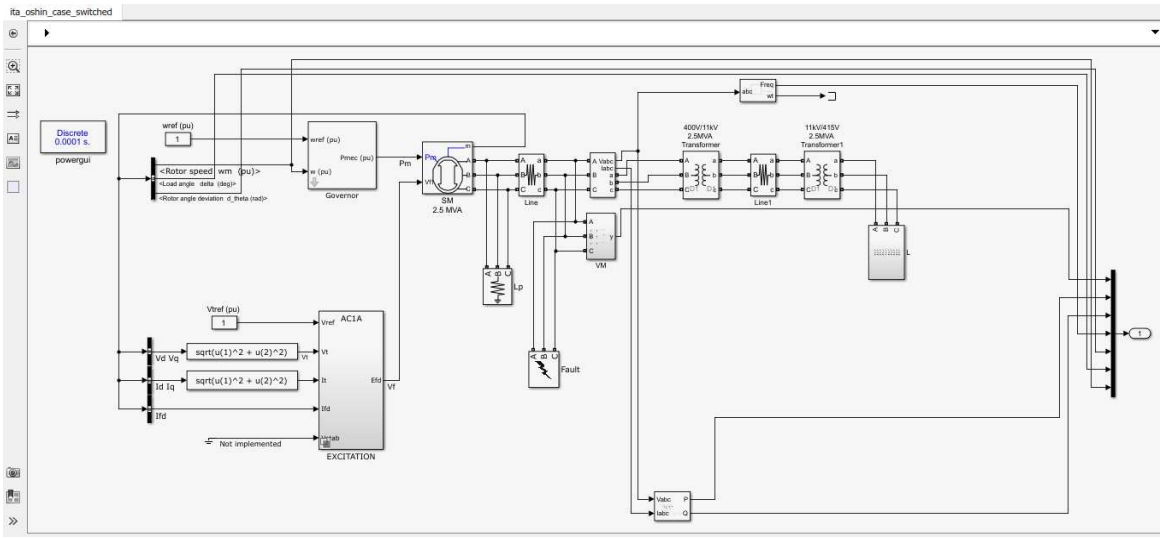

Figure 5: Model for the grid-connected distributed generation system.

With load addition, the system frequency instantaneously deviated from the nominal value of 50Hz and varied from 49.72 to 49.27Hz (-0.56 to -1.46%) for SAM for 10% to 100% load respectively; that of GCM varied from 49.90Hz to 49.44Hz (-0.20% to -1.12%). The instantaneous deviation caused the frequency to oscillate before attaining steady state again after an average recovery time of 4.27s and 3.38s for SAM and GCM respectively.

Voltage responses with gradual load addition

Figures 7a and 7b respectively shows the voltage responses of the distributed generation system in SAM and GCM to gradual load addition. As loads were added, the system voltage to deviated instantaneously from the operational value of 400V and varied from 376 to 232.9V(-6.0 to -41.78% variation) for 10% to 100% load respectively for SAM; 387.7 to 268.3V (-3.08 to -32.93% variation) for GCM. The instantaneous voltage deviation resulted in the oscillation of the voltage before being restored back to steady state after an average recovery time of 13.90s and 4.17s for SAM and GCM respectively.

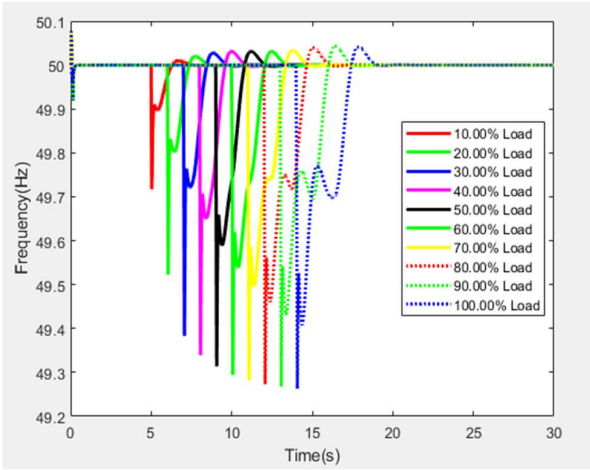

(a)

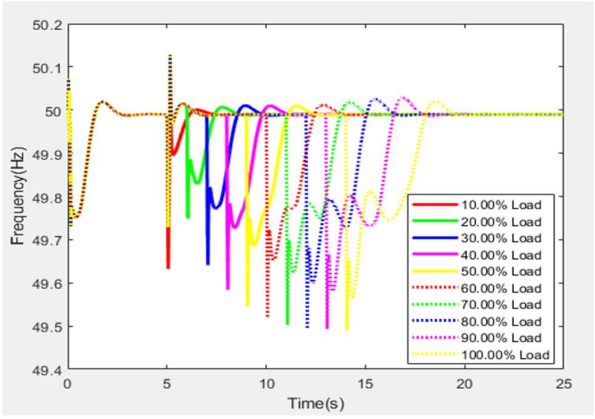

(b)

Figure 6: Frequency responses of the distributed generation system to gradual load addition in (a) stand-alone mode (b) grid-connected mode

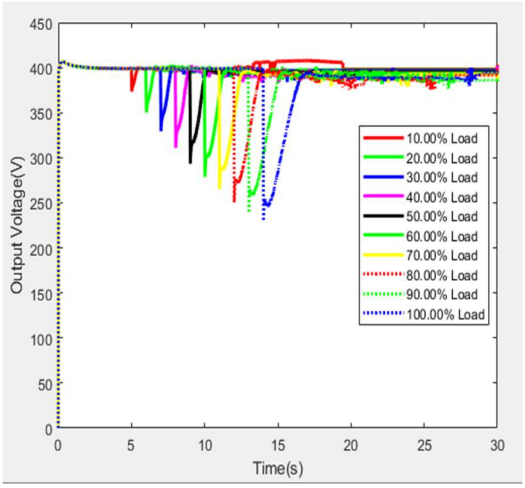

(a)

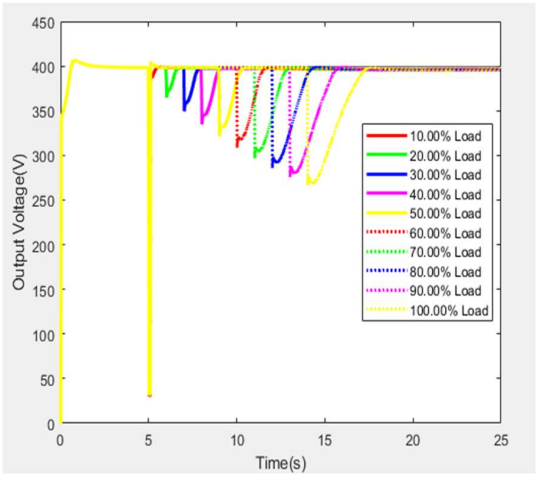

(b)

Figure 7: Voltage responses of the distributed generation system to gradual load addition in (a) stand-alone mode (b) grid-connected mode

Frequency responses to sudden load addition

The frequency responses of the distributed generation system in SAM and GCM to sudden load addition are represented by Figures 8a and 8b respectively. In this case, large loads were suddenly added from 25 to 100 % load which led to sharp instantaneous dip in the frequency which varied from 49.39 to 49.25 Hz (-1.22 to -1.5 %) for 25 to 100% load respectively for SAM; 49.51 to 49.43 Hz for GCM (-0.98 to -1.14 %). However, the frequency was returned to steady state after an average recovery time of 3.86s for SAM and 3.49s for GCM respectively after the dip in value.

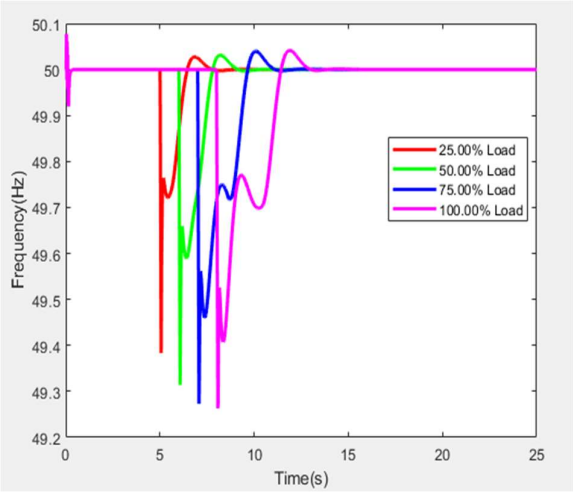

(a)

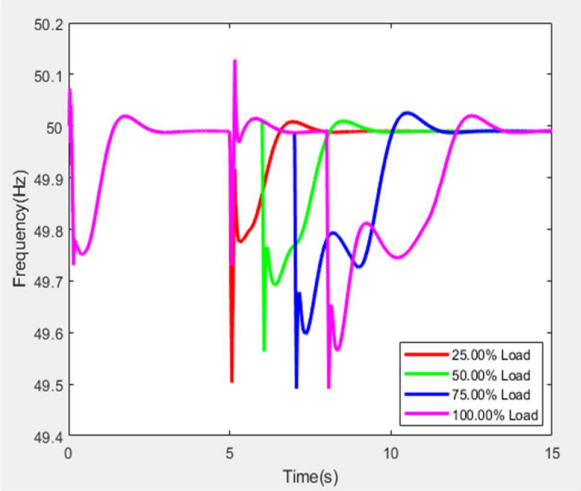

(b)

Figure 8: Frequency responses of the distributed generation system to sudden load addition in (a) stand-alone mode (b) grid-connected mode

Voltage responses

The voltage responses of the DG system in SAM and GCM to sudden load addition can be seen in Figures 9a and 9b respectively. With sudden addition of large loads between 25 to 100% load, there was abnormal and momentary fall in voltage which varied from 271.7 to 190 V (-32.08 to -52.5%) for 25 to 100 % load respectively for SAM; 294.2 to 219.9V(-26.45 to -45.03 %) for GCM.

Despite the fall, the voltage returned to steady state after an average recovery time of 15.81s for SAM and 4.74s for GCM.

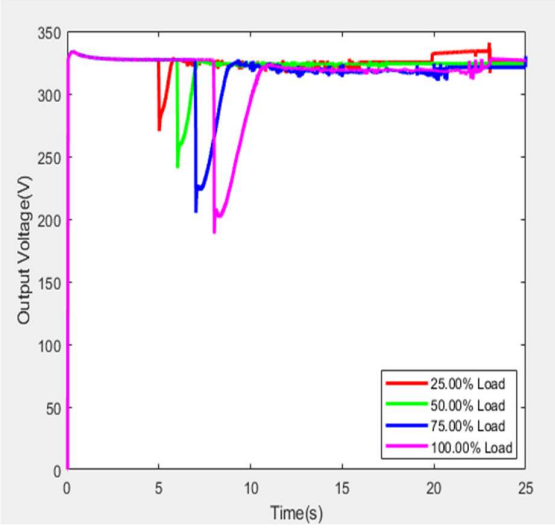

(a)

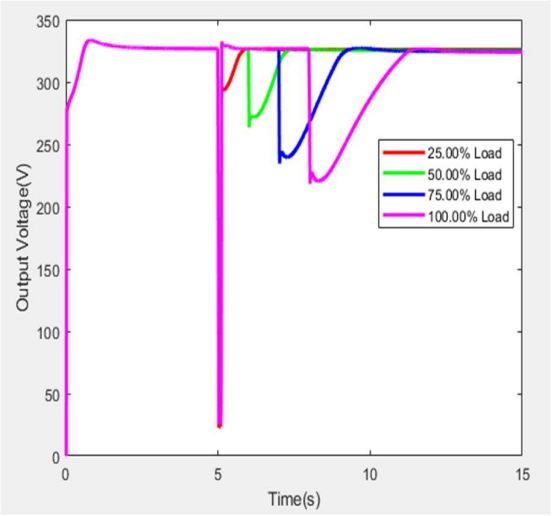

(b)

Figure 9: Voltage responses of the distributed generation system to sudden load addition in (a) stand-alone mode (b) grid-connected mode

It is shown from Figure 10a that for both SAM and GCM, the frequency decreased with gradual increase in load except at 80%, 90% and 100% loads in GCM where the frequency was constant at 49.44Hz. The frequency variation for both SAM and GCM were outside the acceptable operational limit of $\pm 0.5\%$ as stipulated in the grid code for the Nigerian electricity transmission system except at 10% load for GCM which was -0.2%. However, the frequency as shown in the figure is higher and closer to the operational frequency of 50Hz at any load in GCM than SAM.

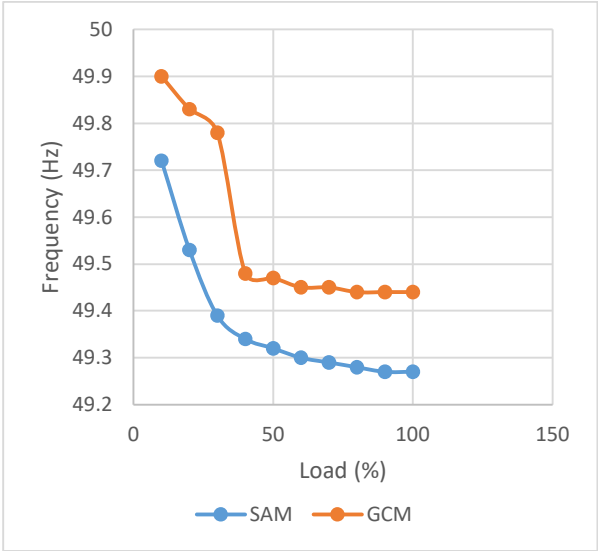

(a)

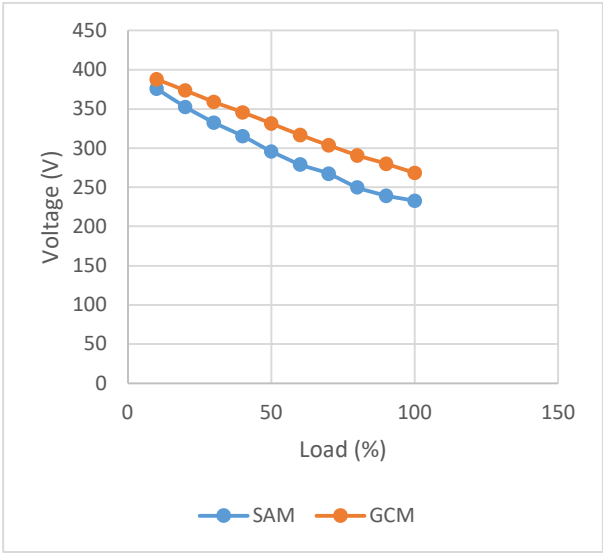

(b)

Figure 10: Comparison of results for gradual load addition for SAM and GCM (a) Frequency (b) Voltage

In Figure 10b the voltage for both SAM and GCM reduced with gradual load addition. The voltage variation for both modes were found to be outside the acceptable operational limit of $\pm 6\%$ as

stipulated in the distribution code for the Nigerian electricity distribution system except at 10% load for both SAM and GCM where the variations were -6.0 and -3.08% respectively. However, the voltage at any load for GCM is higher and closer to the operational voltage of 400V than that of SAM.

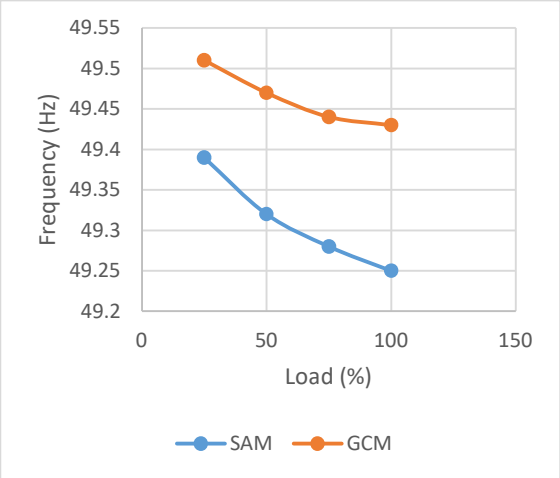

(a)

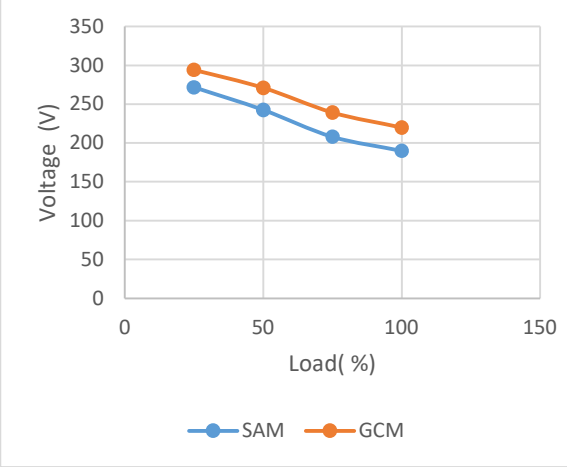

(b)

Figure 11: Comparison of results for sudden load addition for SAM and GCM
(a) Frequency (b) Voltage

From Figure 11a, it is observed that the frequency for both modes reduced with sudden increase in load. The frequency variation for each of SAM and GCM fell outside the allowable operational limit more than what was observed under gradual load addition due to the severity of the sudden load addition. However, the frequency at any load can be seen to be closer to the nominal operational frequency for GCM than SAM.

Figure 11b shows that the more the load was increased, the lesser the voltage. The voltage variation for both modes were discovered to fall well outside the acceptable operational limit far more than what was seen under gradual load addition due to the sudden nature of the load addition. However, the voltage at any load is obviously closer to the nominal operational frequency for GCM than SAM.

CONCLUSION

This paper analyzed the frequency and voltage responses of DG system in SAM and GCM to gradual and sudden load additions. The system was modelled in both SAM and GCM in MATLAB in Simulink environment after which the system was simulated under gradual and sudden load additions. Th results were then analyzed and comparisons were made between the results obtained in SAM and GCM. From the results, the frequency variations with gradual and sudden load additions for the two modes were seen to fall outside the operational limit of 49.75-50.25 Hz (± 0.5 %) except at 10 % load under gradual load addition in GCM. However, the frequency variation of the GCM was discovered to be lesser than that of the SAM either with gradual or sudden load additions. Furthermore, the voltage variations for the two modes under gradual and sudden load additions were found to be outside the acceptable limit of 376-424 V (± 6 %) except at 10 % load for both SAM and GCM which was -0.2%. However, the voltage variation of the GCM was also found to be less than that of the SAM during both gradual and sudden load additions. This study shows that operation of distributed generation system in GCM produced better power quality than in SAM

due to less variations in frequency and voltage with load additions.

REFERENCES

Agbetuyi, A. F., Ademola, A., Orovwode, H. E., Oladipupo O. K., Simeon, M., and Agbetuyi, O. A. (2021). Power Quality Considerations for Embedded Generation Integration in Nigeria: A Case Study of Ogba 33 kV Injection Substation. *International Journal of Electrical and Computer Engineering* 11(2): 956–965.

Chuvychin, V., Sauhats, A., and Strelkovs, V. (2008). Problems of frequency control in the power system with massive penetration of distributed generation. *AT & P journal*: 19-23.

Esan, A. B., Agbetuyi, A. F., Oghorada, O., Ogbeide, K., Awelewa, A. A., and Afolabi, A. E. (2019). Reliability Assessments of an Islanded Hybrid PV-Diesel-Battery System for a Typical Rural Community in Nigeria. *Heliyon* 5(5): 1-14.

Hayerikhiyavi, M., and Dimitrovski, A. (2021). A Practical Assessment of the Power Grid Inertia Constant Using PMUs. 2020 52nd North American Power Symposium (NAPS). Tempe, AZ, USA pp1-5.

Kabalci, E., Boyar, A., and Kabalci, Y. (2021). 2 - Centralized power generation. Hybrid Renewable Energy Systems and Microgrids. Academic Press, London. 521pp.

Kim, M. S., Haider, R., Cho, G. J., Kim, C. H., Won, C. Y., and Chai, J. S. (2019). Comprehensive Review of Islanding Detection Methods for Distributed Generation Systems. *Energies* 12(5): 1-21.

Kothari, D. P., and Nagrath, I. J. (2009). Modern Power System Analysis. Tata McGraw Hill Education Private Limited, New Delhi. 354pp.

Kow, K. W., Wong, Y. W., Rajparthiban, K. R., and Rajprasad, K. R. (2015). Power Quality Analysis for PV Grid Connected System Using PSCAD/EMTDC. *International Journal of Renewable Energy Research* 5(1): 1-13.

Mahmoud, A. A., Hafez, A. A., Yousef, A. M., Gaafar, M. A., Orabi, M., and Ali, A. F. M. (2023). Fault-Tolerant Modular Multilevel Converter for a Seamless Transition between Stand-Alone and Grid-Connected Microgrid. *IET Power Electronics* 16(1): 11–25.

Oladipo, K., Felix, A. A., Bango, O., Chukwuemeka, O., and Olawale, F. (2018). Power Sector Reform in Nigeria: Challenges and Solutions. *IOP Conference Series: Materials Science and Engineering* 413(012037): 1-14.

Patil, K. R., Karnik, S. R., Raju, A. B. (2021). A Comparative Study of DG Impacts on Power System Stability under Equal and Unequal Load Growth Scenarios. *Asian Journal of Convergence in Technology* 7(2): 1-7.

Rudresha, S. J., Ankaliki, S. G., and Ananthapadmanabha, T. (2020). Impact of DG Integration in Distribution System on Voltage Stability and Loss Reduction for Different Loading Conditions. *International Journal of Recent Technology and Engineering (IJRTE)* 8(5): 2177–2181.

Saadat, H. (1999). Power System Analysis. McGraw-Hill Companies, New York. 720pp.

Samala, R. K., and Kotapuri, M. R. (2018). Power Loss Reduction Using Distributed Generation. Modelling, Measurement and Control A. *Journal of International*

Information and Engineering Technology Association (IIETA) 91(3): 104–113.

Salimon, S. A., Adepoju, G. A., Adebayo, I. G., Howlader, H. R., Ayanlade, S. O., and Adewuyi, O. B. (2023). Impact of Distributed Generators Penetration Level on the Power Loss and Voltage Profile of Radial Distribution Networks. *Energies* 16(4): 1-32.

Shokooh, F. (1979). An Explicit State Model of a Synchronous Machine - Transformer - Scr Bridge Unit. [Doctoral Dissertation, Louisiana State University].

Simeon, M., Elizabeth, A., Wara, S. T., Adoghe, A., and Hope, O. (2018). Efficient Energy Management System Using Pir Sensor. 2018 IEEE PES/IAS Power Africa, Power Africa 2018 pp601–606.

Sule, A. H. (2022). Impact of Integration of Renewable Energy Sources on Power System Stability, Fault Protection and Location: A Review. *Direct Research Journal of Engineering and Information Technology* 9(4): 87-100.

Zhang, X., Guo, K., Wang, L., Cong, Y., and Wang, Q. (2023). Analysis of the Influence of Distributed Generation on Distribution Network Voltage. *Journal of Physics: Conference Series* 2418 (012034): 1-7.